Analyst

PAPER

View Article Online
View Journal | View Issue



Cite this: *Analyst*, 2026, **151**, 1669

# Rapid and colorimetric assay for the detection of *S. pneumoniae* based on hydrogen peroxide release and analysis using color image processing

Cagla Celik Yoldas, *[a] Nimet Temur, [b] Nilay Ildiz,[c] Pinar Sagiroglu,[d] Mustafa Altay Atalay,[d] Ali Yilmaz,[e] Ersen Gokturk[f] and Ismail Ocsoy [b]

Although *Streptococcus pneumoniae* (*S. pneumoniae*) is routinely identified using various clinical methods, most existing techniques are complicated, time-consuming, and require expensive equipment. Consequently, there is a critical need for rapid, sensitive, and economical detection methods. Herein, we report a rationally designed colorimetric assay incorporating biocompatible anthocyanins for the rapid detection of *S. pneumoniae via* the naked eye and image processing software. Unlike conventional anthocyanin-based assays that rely on pH-dependent color changes, our approach uses anthocyanins as oxidative degradation probes rather than pH indicators. The detection mechanism relies on the oxidative degradation of anthocyanins by hydrogen peroxide ($H_2O_2$), a key virulence factor secreted by *S. pneumoniae*, which induces a distinct color shift to gray. We systematically evaluated the performance of this assay in various matrices, including growth medium, saline solution, and artificial cerebrospinal fluid (aCSF). Bacterial suspensions of 1.0 and 1.5 McFarland were colorimetrically detected within 90 and 30 minutes, respectively, through naked-eye observation and Delta-E analysis. This study demonstrates a highly stable, cost-effective, and easy-to-prepare diagnostic tool that offers significant advantages over traditional methods for point-of-care testing.

Received 24th December 2025,
Accepted 12th February 2026

DOI: 10.1039/d5an01356a

rsc.li/analyst



## 1. Introduction

Infections caused by *Streptococcus pneumoniae* (*S. pneumoniae*) are a major global health concern, significantly increasing morbidity and mortality, particularly among young children and the elderly.[1,2] Pneumococci can cause mild respiratory tract infections, such as otitis and sinusitis, as well as more serious, life-threatening situations, such as septicemic or non-septicemic pneumonia and meningitis. They can also induce invasive pneumococcal diseases by spreading into the bloodstream and brain. While 33 different types of *S. pneumoniae* led to 1.2 million deaths and 197 million cases of pneumonia worldwide, an estimated 829 000 deaths were caused by pneumococcus in 2019, 225 000 of which occurred in children under five years old.[3,4] Researchers uncovered that pneumococci were associated with the highest number of deaths in young children.[1,4] Following the emergence of SARS-CoV-2, *S. pneumoniae* has been the most frequently observed co-infecting organism with SARS-CoV-2 in patients.[5] In the 2024 Bacterial Priority Pathogens List (BPPL) published by the World Health Organization (WHO), macrolide-resistant Group A Streptococci and penicillin-resistant Group B Streptococci were added to the list for the first time. In addition to that pneumococci were identified as one of the 24 priority pathogens requiring urgent new antibiotics in the final ranking of antibiotic-resistant bacteria in the 2024 WHO BPPL.[6]

It is vitally important to quickly and correctly treat infections associated with *S. pneumoniae* in order to normalize the critical situation. In most clinical laboratories, *S. pneumoniae* is typically identified through characteristic phenotypes, including microscopic morphology (light-pointed, cocci-shaped, Gram-positive bacteria that are usually found in pairs), colony morphology, α-hemolysis observed on blood agar, catalase negativity, optochin sensitivity and bile solubility.[7] Traditional pathogen detection methods also include microbial culture, molecular biology detection and immunological tests.[8] Although microbial culture is the gold standard method, the procedure is complex and time-consuming (3–5 days). This is not suitable for the rapid on-site detection and

[a]*Department of Analytical Chemistry, Faculty of Pharmacy, Harran University, 63050 Sanliurfa, Türkiye. E-mail: caglacelik@harran.edu.tr*
[b]*Department of Analytical Chemistry, Faculty of Pharmacy, Erciyes University, 38039 Kayseri, Türkiye*
[c]*Medical Imaging Department, Vocational School of Health Services, Bandirma Onyedi Eylul University, 10200 Balikesir, Türkiye*
[d]*Department of Medical Microbiology, Faculty of Medicine, Erciyes University, 38039 Kayseri, Türkiye*
[e]*Department of Neurosurgery, Faculty of Medicine, Ordu University, 52200 Ordu, Türkiye*
[f]*Department of Chemistry, Hatay Mustafa Kemal University, Hatay, 31001, Türkiye*

primary screening of bulk samples.[9] Molecular biology detection technology is more sensitive, but requires sensitive equipment and professional technicians.[10] Immunological detection methods based on antibody technology are simple, fast, and widely used for the rapid detection of pathogens; however, these methods require immune animals and high cost.[11] Therefore, new strategies are highly needed to increase detection efficiency and sensitivity to reduce detection time and cost. Colorimetric tests based on different mechanisms have been developed for the detection, classification and resistance analysis of various bacterial species.[12–14] However, the inadequacy of routine phenotyping methods in detecting *S. pneumoniae*, particularly in clinics, highlights the importance of developing new strategies.

*S. pneumoniae* uses a number of virulence factors to successfully adhere to host cells, evade the immune system, and overcome the epithelial barrier. One of the *S. pneumoniae* virulence factors is hydrogen peroxide ($H_2O_2$), which is primarily produced by pneumococcal pyruvate oxidase (spxB) as a byproduct of acetyl-pyruvate production. The absence of the catalase enzyme, which breaks down $H_2O_2$, produced by the effect of spxB in *S. pneumoniae* leads to its accumulation. During pneumococcal infection, $H_2O_2$ has been shown to induce DNA damage and apoptosis in alveolar epithelial cells.[15,16] Inspired by this information, we propose an anthocyanin-incorporated colorimetric diagnostic test by utilizing $H_2O_2$ as a main virulence factor of *S. pneumoniae*. The previous studies demonstrated how we colorimetrically detect organic acidic volatile compounds, which acidified the growth medium, released by bacteria with anthocyanin based tests.[17–23] We used anthocyanins as natural pH indicators for colorimetric detection of target bacteria based upon pH changes in the microenvironment. The anthocyanin molecules appear pink, purple and blue/greenish/yellow in acidic, neutral and alkaline test media, respectively. Additionally, anthocyanin molecules can be degraded when exposed to high temperatures, $H_2O_2$, sulphites, enzymes and light.[24–26]

Here, we, for the first time, rapidly and colorimetrically detect *S. pneumoniae* by the naked eye and color image processing software through released $H_2O_2$ molecules. The $H_2O_2$ produced by *S. pneumoniae* causes the degradation of anthocyanin molecules in test media, which triggers the change of their initial colors to colorless or gray. This test demonstrates that the *S. pneumoniae* virulence factor $H_2O_2$ can be directly, quickly, accurately and economically detected. To semi-quantitatively support colorimetric test results, they were analyzed using color image processing techniques. We propose that this test is considered a significant step in the struggle against infectious diseases.

## 2. Materials and methods

### 2.1. Materials and instrumentations

Tryptic soy agar (Merck, Germany), skimmed milk medium (Difco, USA), meat extract (Acumedia, UK), NaCl, KCl, $NaH_2PO_4$, $CaCl_2$, $MgSO_4$, $NaHCO_3$ (Isolab, Türkiye), and peptone (Mast Diagnostic, UK) were all purchased from the companies indicated.

Microorganisms: *S. pneumoniae* ATCC 49619, *Staphylococcus aureus* (*S. aureus*) ATCC 29213, *Enterococcus faecium* (*E. faecium*) ATCC 8459, *Enterococcus faecalis* (*E. faecalis*) ATCC 29212, *Klebsiella pneumoniae* (*K. pneumoniae*) ATCC 700603, *Escherichia coli* (*E. coli*) ATCC 25922, *Streptococcus agalactiae* (*S. agalactiae*) ATCC 12401, and *Streptococcus pyogenes* (*S. pyogenes*) ATCC 19615 were obtained from Bandirma Onyedi Eylul University, Vocational School of Health Services, Pharmaceutical Microbiology Research Laboratory ATCC culture collection. All bacterial strains were stored in a skim milk medium at −20 °C and regenerated in triptic soy agar prior to the experiments. The optical density ($OD_{600}$) of bacterial suspensions in saline and artificial cerebrospinal fluid (aCSF) was determined using a spectrophotometer (Azure Ao, Azure Biosystems, Inc.). To ensure quantitative accuracy, the inoculum density was verified spectrophotometrically rather than relying solely on visual estimation. For the primary inoculum (0.5 McFarland), an $OD_{600}$ value of 0.089 was measured, corresponding to $1.35 \times 10^8$ CFU $mL^{-1}$. The correlation was further verified at other turbidity levels; 0.2, 1.0, and 1.5 McFarland standards corresponding to calculated concentrations of $6.1 \times 10^7$ ($OD_{600}$ = 0.089), $2.7 \times 10^8$ ($OD_{600}$ = 0.18), and $4.5 \times 10^8$ ($OD_{600}$ = 0.30) CFU $mL^{-1}$, respectively. All bacterial cultivations and related assays involving *S. pneumoniae* were performed in a certified Biosafety Level 2 (BSL-2) laboratory. Standard microbiological practices and sterile protocols, such as the autoclaving of biohazardous waste, were strictly adhered to in order to ensure laboratory safety.

### 2.2. Red cabbage (*Brassica oleracea*) extraction

Red cabbage (*Brassica oleracea* L., Brassicaceae) is a natural source of anthocyanins, compounds that interact with $H_2O_2$ in a test medium. These anthocyanins are glycosides of 2-phenylbenzopyrylium or flavilium salts, which have a C6–C3–C6 carbon skeleton structure with hydroxyl and/or methoxy derivatives. The primary anthocyanins found in Brassica plants are cyanidin 3-diglucoside-5-glucoside derivatives that are esterified with various aromatic and aliphatic acids, as well as with glucosides and xylose. Red cabbage is extracted to obtain anthocyanins. In the first step, the purple leaves are separated from the cabbage, washed and dried. The dried leaves are cut into small pieces. One hundred grams of the cut leaves are boiled in 100 mL of distilled water for 30 minutes (min). After this 30 min period, the extracted purple solution is filtered through Whatman No. 1 filter paper. The filtered anthocyanin solution was transferred to amber glass bottles to protect against photodegradation and stored at 4 °C.[27,28] Under these conditions, the probe remained chemically and functionally stable for at least 30 days (SI, Fig. S1).

### 2.3. Preparation of colorimetric tests

We performed the colorimetric tests using anthocyanin in the solution form with minor modifications from our previous

 

studies.[17–20,24] Briefly, in the first step, 40 g $L^{-1}$ peptone, 4 g $L^{-1}$ meat extract and 300 g $L^{-1}$ salt were sterilized in an autoclave at 121 °C for 15 min to prepare the 4X growth medium (GM). In the second step, the red cabbage extract was diluted with distilled water to achieve a standardized optical density (Abs ~ 1.0, corresponding to approx. 20% v/v) to ensure constant anthocyanin concentration, as characterized by the UV-Vis spectrum (Fig. S2). Subsequently, the pH of this standardized solution was adjusted to 8.0 and 11.0 using 1 M NaOH solution. The blue and green anthocyanin solutions were sterilized using a filter. In the third step, bacterial suspensions were prepared using saline or aCSF and adjusted using a McFarland densitometer.

For 10X aCSF, 73.05 g NaCl, 1.86 g KCl, 1.44 g $NaH_2PO_4$, 22.52 g D-glucose, 2.94 g $CaCl_2$, and 4.93 g $MgSO_4$ were dissolved in 1 L of distilled water. Prior to use, to 100 ml of the stock solution, 800 ml of distilled water was added. Then, 2.18 g of $NaHCO_3$ was added and dissolved, the volume was adjusted to 1 L and the pH was adjusted to 7.3 with 12 N HCl. The sterilization process was performed using a sterile filter.[29] During the test procedure, 75 μL each of GM and anthocyanin solution (at pH 8 or 11) were added to the test wells, followed by 150 μL of bacterial suspension. This mixture constituted the test medium, containing 1X GM and a 5% anthocyanin solution. The test wells were incubated at 37 °C and the color change over time was recorded.

For the translation of this assay into a clinical diagnostic tool, the following standardized protocol is proposed based on our optimized experimental conditions. The colorimetric array consists of 75 μL of GM (to facilitate rapid bacterial metabolism and $H_2O_2$ release) and 75 μL of anthocyanin adjusted to pH 8, as this pH level provided the optimal reaction kinetics compared to pH 11. To this mixture, 150 μL of the aCSF was added. The test was incubated at 37 °C, and the diagnostic readout was obtained within 90 min *via* naked-eye observation or smartphone analysis. All chemical reagents, including $H_2O_2$ solutions and anthocyanin extracts, were handled in accordance with institutional safety guidelines. Appropriate personal protective equipment, such as gloves and safety goggles, was used throughout the experiments to prevent accidental exposure.

### 2.4. Digital image processing

We used digital image processing for the semi-quantitative analysis of colorimetric test results, in addition to visual monitoring of color changes. Test wells were recorded over time using a white background. Changes in the color of the test wells were analyzed using ImageJ software (National Institutes of Health). ImageJ software was used to analyze the Red, Green and Blue values in the test wells. Using these data, the formation of a gray color in blue or green test wells due to *S. pneumoniae* strains was calculated. While other pathogens turn the blue test medium pink or purple, Red/Blue and Delta-E values were calculated to demonstrate the formation of a gray color by pneumococci. The rate of decrease in the blue value was monitored using the R/B value, while the difference between the two colors was measured by the Delta-E analysis. Delta-E (DE), calculated according to the CIE 1976 Lab formula, was used to measure the difference between the initial color and the color at the end of incubation.[30,31]

$$\Delta E = [(\Delta L)^2 + (\Delta a)^2 + (\Delta b)^2]^{1/2} \quad (1)$$

Delta-E values are calculated based on the three fundamental differences defined in formula (1): $\Delta L$, $\Delta a$ and $\Delta b$. These three elements define the dimensions of the CIE Lab color space. $\Delta a$ represents the difference between red and green, $\Delta b$ represents the difference between yellow and blue, and $\Delta L$ represents the difference between black and white. These differences are low in similar images and high in different ones. This helps to demonstrate color change.[32,33] Thanks to this analysis, the color difference in the test wells can be analyzed more accurately than by the human eye alone. The integration of digital image processing significantly reduces the dependency on specialized personnel. Unlike traditional culture methods that rely on the subjective visual assessment of the colony morphology by experienced microbiologists, this assay utilizes a computational algorithm to calculate the color difference (Delta-E). This objective readout minimizes personnel errors and standardizes the diagnostic decision, making the technology adaptable for future mobile-app integration and use by non-expert personnel.

## 3. Results and discussion

In this current work, anthocyanin groups used as a natural pH indicator in colorimetric diagnostic tests were extracted from red cabbage extract (RCE). It is worth mentioning that anthocyanin groups have advantages over other synthetic pH-responsive dyes owing to their biocompatibility, approval by the Food and Drug Administration (FDA), wide color spectrum, cost-effectiveness and easy accessibility.[24,34,35]

The color of anthocyanin molecules can change based on the pH value (pH) of the reaction environment through the protonation and deprotonation of hydroxyl groups on the anthocyanin structure.[17,18] In this work, $H_2O_2$ released from *S. pneumoniae* causes oxidative degradation of anthocyanins, and then the initial color of anthocyanins in the test solution turns gray and colorless based on the amount of $H_2O_2$ (Scheme 1).

The production of $H_2O_2$ does not drastically change the pH value of the reaction environment. The color change mechanism of anthocyanin molecules relies on their degradation instead of protonation or deprotonation. We showed how different concentrations of $H_2O_2$ influence the color of anthocyanin solutions, as given in Fig. S3. The anthocyanin solutions were prepared at pH 8 with blue color, then various concentrations of $H_2O_2$ (0.1 mM, 0.5 mM, 1 mM, 10 mM, 100 mM and 1000 mM) were added to each anthocyanin solution and the mixtures were incubated for 180 min (Fig. S3A). The anthocyanin solution without the addition of $H_2O_2$ exhibited great stability by maintaining its initial blue color. The addition of 0.1 mM $H_2O_2$ changed the color of the anthocyanin solution

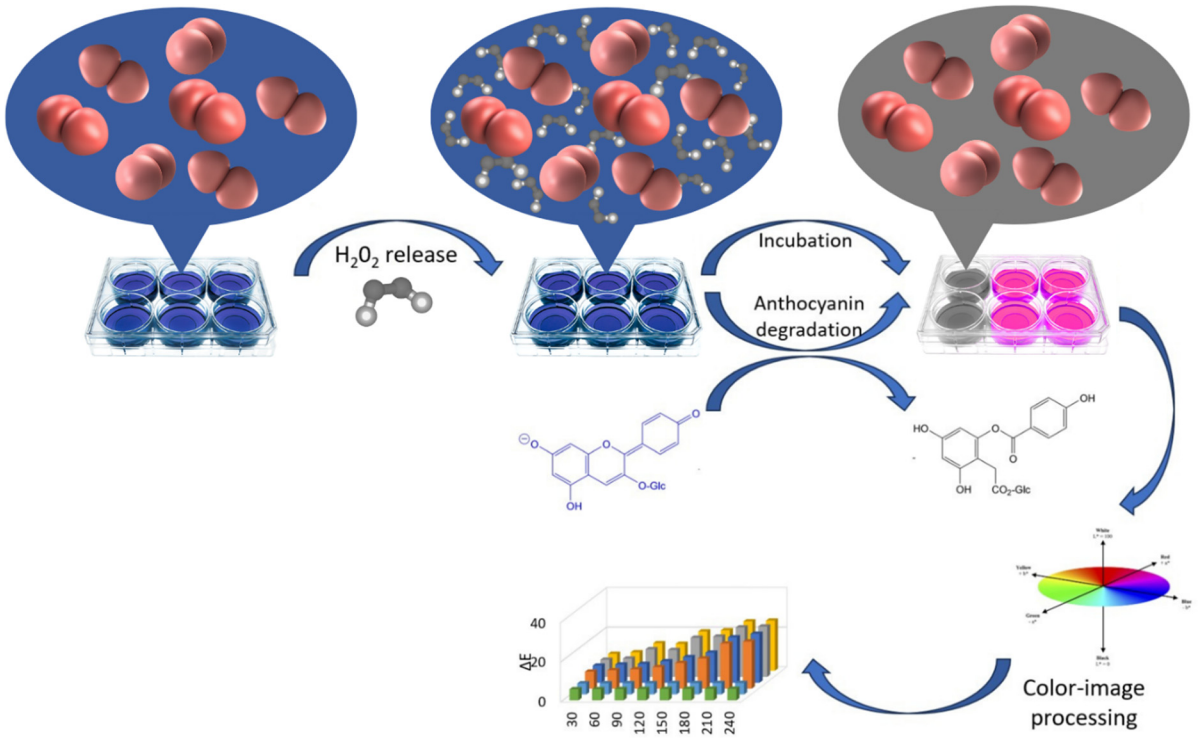


**Scheme 1** Schematic illustration of the rapid and colorimetric assay for the detection of *S. pneumoniae* based on $H_2O_2$ release and analysis using color image processing.

from blue to purple in 30 min of incubation. The color of the anthocyanin solution turned greenish in the presence of both 0.5 mM and 1 mM $H_2O_2$ in 30 min of incubation. The addition of 10 mM, 100 mM and 1000 mM $H_2O_2$ in anthocyanin solutions changed their color from blue to yellowish in 20 min, 5 min and initial incubation times, respectively. Quantitative analysis revealed an exponential correlation between the $H_2O_2$ concentration and the Delta-E values at 30 min (Fig. S3B), confirming that the sensing signal is directly driven by the stoichiometry of the peroxide-mediated degradation.

We demonstrate how $H_2O_2$ concentrations affect the pH of $H_2O_2$ itself and anthocyanin solutions prepared at pH 8 and pH 11, as presented in Fig. S4. For instance, the pH values of the $H_2O_2$ itself with a series of concentrations including 0.1 mM, 0.5 mM, 1 mM, 10 mM, 100 mM and 1000 mM were measured. At the lowest and highest $H_2O_2$ concentrations, the pH values of the $H_2O_2$ solution were determined to be 8.17–6.40. The decrease in pH at the highest $H_2O_2$ concentration can be attributed to autoprotolysis of $H_2O_2$ molecules. While the pH values of anthocyanin solutions prepared at pH 8 and pH 11 were found to be 7.10 and 7.65 at the lowest $H_2O_2$ concentration, the highest $H_2O_2$ concentration decreased their pH to 6.13 and 6.62, respectively. Although anthocyanin solution exhibits a purple color between pH 7 and pH 5, indicating that no color change is observed in this pH range, $H_2O_2$ at certain concentrations exhibits a change in the color of its solution from the initial color to gray color.

As we discussed above, *S. pneumoniae* is a catalase-negative bacterium, and $H_2O_2$ produced by *S. pneumoniae* can accumulate in the air sacs of the lungs owing to the absence of the catalase enzyme and cause DNA damage and apoptosis in alveolar epithelial cells. Although $H_2O_2$ production has an adverse effect on the human body, it is utilized as an indicator for colorimetric detection of *S. pneumoniae* using the test we developed in this study. We prepared a blue colored anthocyanin solution in saline at pH 8, then, the blue color of the solution disappeared in 10 min after the addition of 300 mM $H_2O_2$, which degraded the structure of anthocyanin (left one in Fig. 1). To show how the presence of the catalase affects the detection of $H_2O_2$, 1000 U

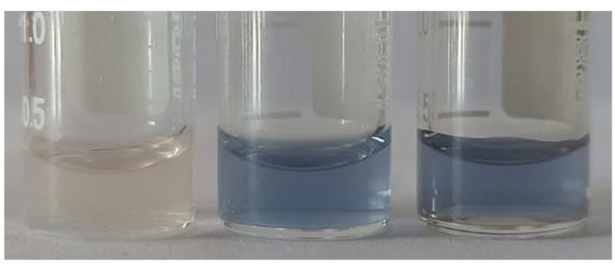


**Fig. 1** Color change of anthocyanin in the presence of $H_2O_2$ or catalase and $H_2O_2$.

$mL^{-1}$ catalase was added to the anthocyanin solution mentioned above, and expectedly the blue color of the solution did not change owing to the breaking down of $H_2O_2$ to $H_2O$ by the catalase (middle one in Fig. 1). We already mentioned that anthocyanin solution is quite stable and maintains its initial blue color in the absence of $H_2O_2$, acid or basic molecules (right one in Fig. 1).

A possible oxidation mechanism of the flavylium ion by $H_2O_2$ is demonstrated in Fig. 2. Anthocyanins are known to exist as mixtures of **A** and **B** structures in chemical equilibrium in water due to the reversible hydration at position 2 of the middle ring.[36] Treatment of the **B** structure with $H_2O_2$ generates a highly unstable hemiketal structure (**C**).[36–38] Rearrangement of **C** gives a glucose ester (**D**). Hydrolysis of the compound **D** in water produces protocatechuic acid **E** and compound **F**.[36–38]

The blue colored test solution was prepared using 5% anthocyanin, growth medium at pH 8 and placed in the 1st column of the well. *S. pneumoniae* suspensions at different concentrations in a saline solution (0.2 McFarland, 0.5 McFarland 1.0 McFarland and 1.5 McFarland) were separately added to each 1st column and incubated for various periods of time (Fig. 3A). We demonstrated that the initial blue color of the test solutions in the 1st columns of the well-plates became gray in the presence of the *S. pneumoniae* suspensions. While the gray color of the test solutions containing 1.0 McFarland and 1.5 McFarland *S. pneumoniae* suspensions appeared first in 90 min, 0.2 McFarland and 0.5 McFarland *S. pneumoniae* suspensions gave a gray color at the end of the 210 min incubation time. We propose that obtaining a gray color in the short incubation time is proportional to high concentration of *S. pneumoniae*, which produces more $H_2O_2$. In terms of stability control, the 2nd column and 3rd column containing 5% anthocyanin + growth medium and 5% anthocyanin + saline solution, respectively, maintain their original blue color in the absence of *S. pneumoniae* (Fig. 3A). We believe that the test solutions used for the control experiment are quite stable owing to no changes in their original blue color. In order to quantitatively support colorimetric results observed by the naked eye, R/B and Delta-E analyses were performed. While the R/B values of the test solution in the 1st column showed a significant increase based on the concentration of *S. pneumoniae* suspensions and incubation time, no difference in R/B values for the 2nd column and 3rd column was observed regardless of the incubation time owing to the absence of *S. pneumoniae* (Fig. 3B). Expectedly, although the first color change seen by the naked eye was in the 1st column at 90 min of incubation in the presence of 1.0 McFarland and 1.5 McFarland *S. pneumoniae* suspensions, increases in the R/B values were recorded at 60 min of incubation with the same bacterial concentrations. In addition to this, the $\Delta E$ analysis for the two colors showed larger differences between each other, providing more accurate detection of *S. pneumoniae* (Fig. 3C).

In order to examine the effect of the initial color of the test solution on the detection of *S. pneumoniae*, we prepared a test solution with a green color at pH 11 by keeping all contents the same as given in Fig. 4A. The green color test solutions were placed in the 1st column of each well-plate, and then we observed the color change depending on the concentration of *S. pneumoniae* and incubation times (Fig. 4).

As is seen, the initial green color of the test solutions in the 1st columns of the well-plates turned gray in 150 min in the presence of 1.0 McFarland and 1.5 McFarland *S. pneumoniae* suspensions. However, low concentrations of *S. pneumoniae* suspensions (0.2 McFarland and 0.5 McFarland) changed the color of the test solutions to gray at incubation times of 210 min and 240 min. We claim that a high concentration of *S. pneumoniae* leads to an increase in $H_2O_2$ production, resulting in rapid anthocyanin degradation and eventual color change. The initial green color of the test solutions in the 2nd column and the 3rd column was constant during the incubation owing to the absence of the *S. pneumoniae* suspension, as presented in Fig. 4A.

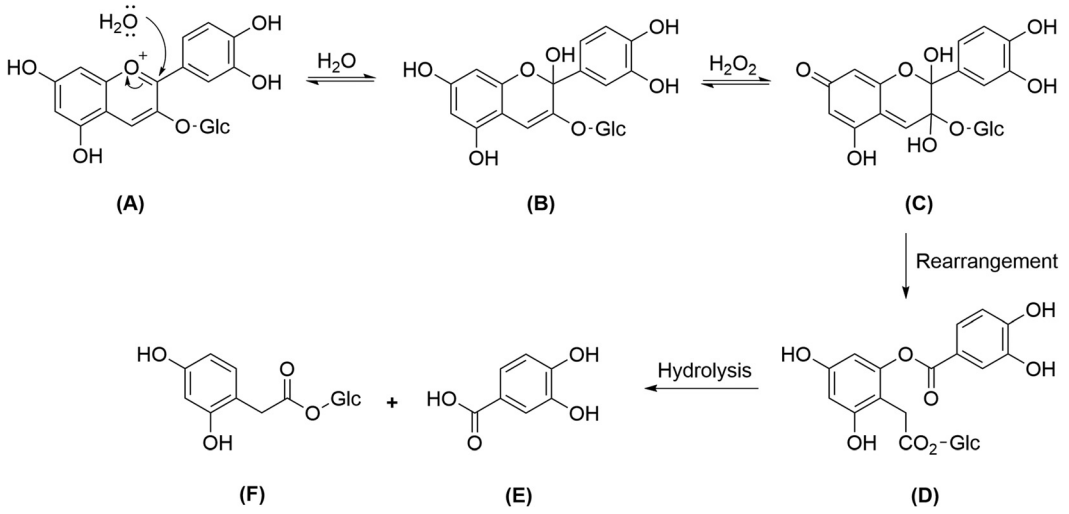


Fig. 2 Proposed oxidation mechanism of the flavylium ion by $H_2O_2$.

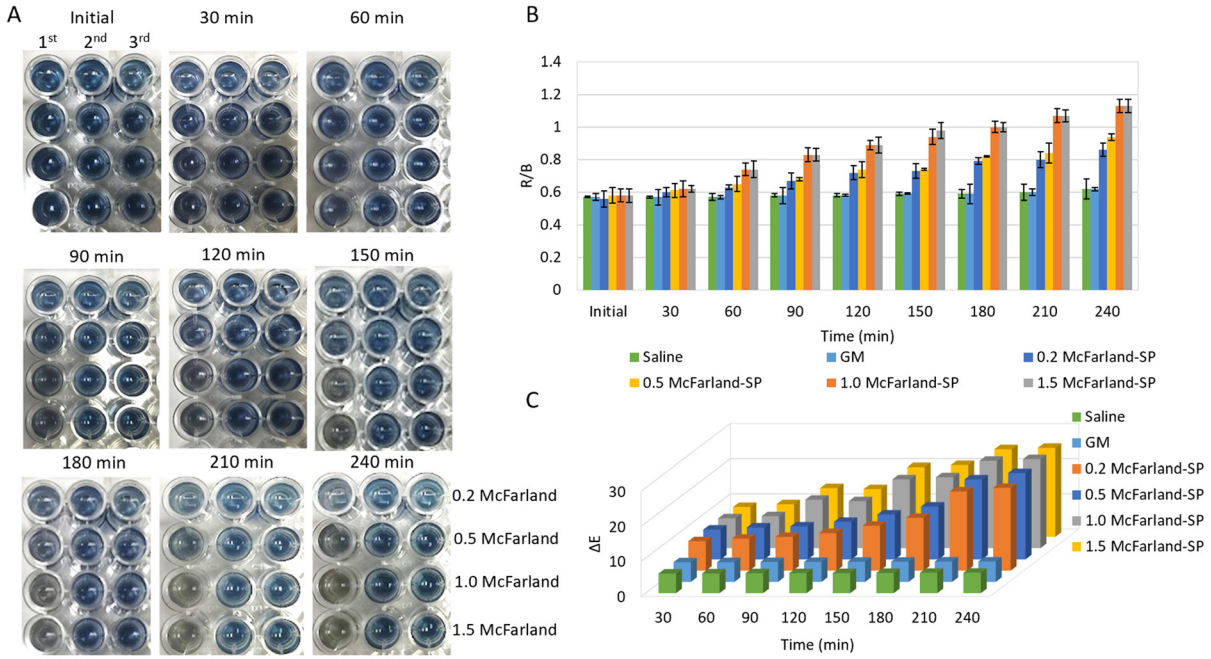


**Fig. 3** (A) Blue colorimetric array was prepared at pH 8 and incubated for different periods of time with different concentrations of *S. pneumoniae*, (B) R/B analysis and (C) Δ*E* analysis. The bar charts illustrate the progressive increase in signal intensity (R/B and Delta-E) over time, clearly distinguishing the positive samples from the saline and GM wells at each interval. The error bars represent standard deviation (SD) generated from three measurements ($n$ = 3) (raw data provided in Table S1). (Note: 0.2, 0.5, 1.0, and 1.5 McFarland correspond to $6.1 \times 10^7$, $1.35 \times 10^8$, $2.7 \times 10^8$, and $4.5 \times 10^8$ CFU mL$^{-1}$, respectively).

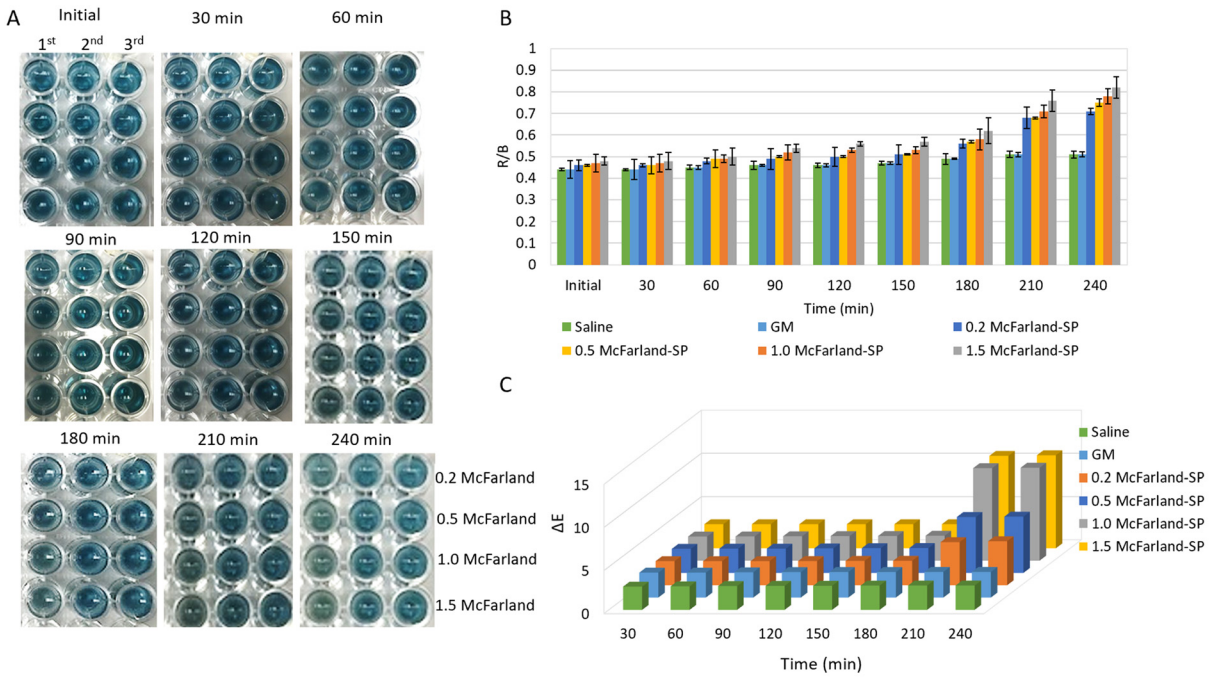


**Fig. 4** (A) Green colorimetric array was prepared at pH 11 and incubated for different periods of time with different concentrations of *S. pneumoniae*, (B) R/B analysis and (C) Δ*E* analysis (raw data provided in Table S2). (Note: 0.2, 0.5, 1.0, and 1.5 McFarland correspond to $6.1 \times 10^7$, $1.35 \times 10^8$, $2.7 \times 10^8$, and $4.5 \times 10^8$ CFU mL$^{-1}$, respectively).

The color changes witnessed by the naked eye were consistent with R/B and $\Delta E$ analysis. While an increase in R/B and difference in $\Delta E$ values were first obtained after 150 min of incubation time, the much clear and distinct differences between R/B and $\Delta E$ values were revealed after 210 min and 240 min of incubation, as given in Fig. 4B and C. We interpret that the blue color test solution gave a much rapid colorimetric response, as analyzed by both the naked eye and digital imaging process in the presence of the same concentration of *S. pneumoniae* suspensions, compared to the green color test solution owing to the initial color of the test solution (since green color is close to gray color) and degradation performance of anthocyanin molecules.

We further performed a comparative study to observe the colorimetric response of the test solution against several bacterial suspensions including *S. pneumoniae* (SP), *S. aureus* (SA), *E. faecium* (EFm), *E. faecalis* (EFs), *K. pneumoniae* (KP) and *E. coli* (EC). For instance, we prepared blue and green color tests in saline solutions, and they were separately placed in the first two rows (1$^{st}$ and 2$^{nd}$) and the last two rows of the well-plate (3$^{rd}$ and 4$^{th}$) as shown in Fig. 5A. The columns of the well-plate were labeled accordingly. Each column of the well-plate contains the same test solution content and different bacterial suspensions at different concentrations (1$^{st}$ column: SP, 2$^{nd}$ column: SA, 3$^{rd}$ column: EFm, 4$^{th}$ column: EFs, 5$^{th}$ column: KP, and 6$^{th}$ column: EC), and the 7$^{th}$ column contains only the test solution. As we expected, for the blue color test solution in the 1$^{st}$ column, the color rapidly changed to gray color compared to the green color test solution in the presence of SP. Both blue and green color test solutions in the 3$^{rd}$, 4$^{th}$, 5$^{th}$ and 6$^{th}$ columns changed to pink color solutions in the presence of EFm, EFs, KP and EC suspensions. These bacterial suspensions produce acidic organic volatile compounds as part of their growth process and make the micro-environment of each column acidic in which anthocyanin molecules are protonated, and then the color change occurs. Although the 2$^{nd}$ column includes SA, only the blue color test solution changed to a pink-purple like color solution in 210 min of incubation. We assume that SA bacterial cells were not efficiently grown, so no rapid and distinct color change was observed. The 7$^{th}$ column has only blue and green color test solutions without bacterial suspensions, and shows great stability of the test solutions by maintaining their initial colors. Fig. 5B and C show R/B values of each well, and the increase in each R/B value is related to the color change of the test solution, especially the blue color test solution. We systematically prepared blue and green test solutions in aCSF, and the experiments shown in Fig. 5 were performed as presented in the SI (Fig. S5). The detection performance for target bacteria was almost the same as that of the test solutions prepared in saline solution and CSF. However, the growth rate of SA in the 2$^{nd}$ column was much faster in CSF than in saline solution, which directly influences clear and rapid color change of the test solutions.

In terms of further experiments, we prepared the blue and green test solutions and used them for the detection of types

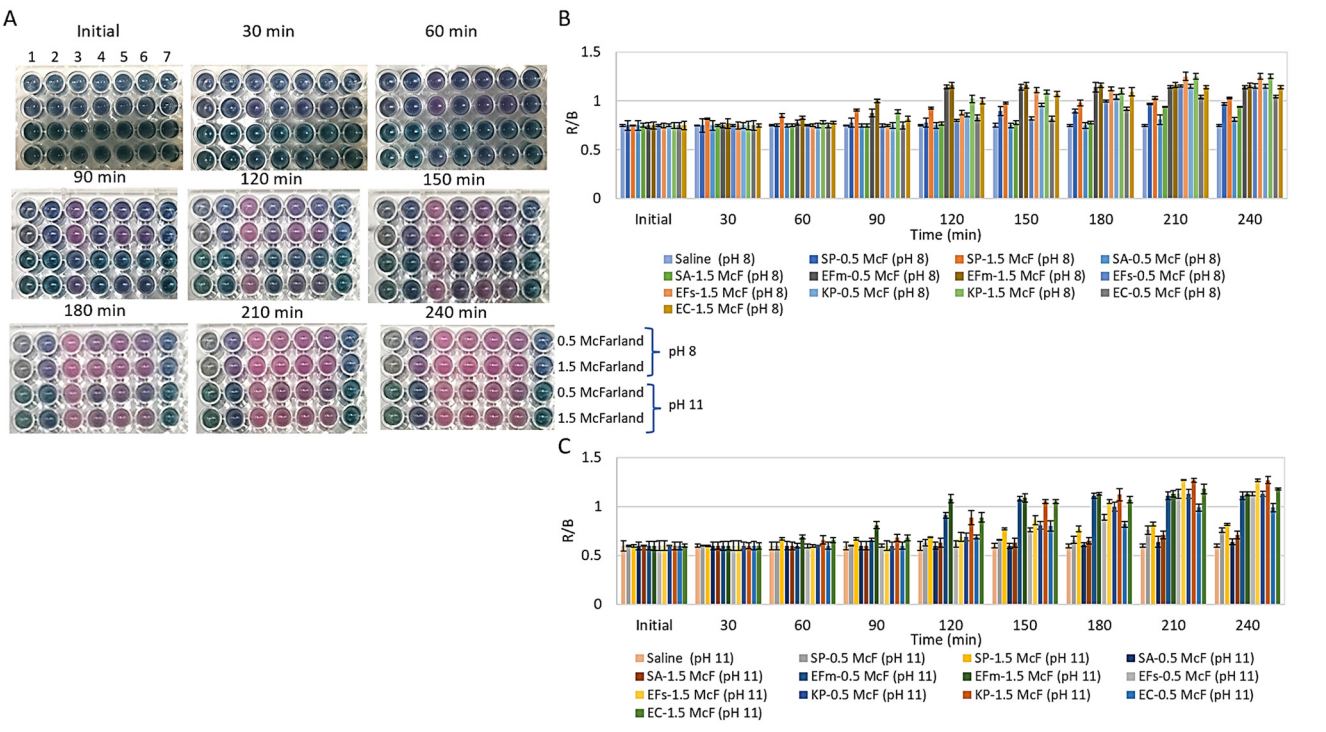


**Fig. 5** (A) Blue and green colorimetric arrays were prepared at pH 8 and pH 11 and incubated for different periods of time with different bacterial pathogens in saline, (B) R/B analysis of the blue (pH 8) colorimetric array and (C) the green (pH 11) colorimetric array (raw data provided in Tables S3 and S4). (Note: 0.5 and 1.5 McFarland correspond to $1.35 \times 10^8$ and $4.5 \times 10^8$ CFU mL$^{-1}$, respectively).

of *Streptococcus* strains like *S. pneumoniae* (SP), *S. agalactiae* (SAg), and *S. pyogenes* (SPy). Fig. 6A shows that only SP suspensions in the 1st column changed the test solution colors to gray; however, the SAg and SPy suspensions in the 2nd and 3rd columns, respectively, caused a pink color owing to the production of acidic organic volatile compounds. We conclude that the anthocyanin solution gives a gray color through the degradation mechanism of anthocyanin only in the presence of SP suspensions. In contrast to that, the anthocyanin solution turned pink regardless of the initial color due to the pH-dependent protonation mechanism in the presence of SAg and SPy suspensions. The R/B values for the blue and green test solutions were calculated as shown in Fig. 6B and C, respectively. The increases in R/B values are well-consistent with the colorimetric results given in Fig. 6A. We show that the change of both test solutions to pink solutions caused by SAg and SPy suspensions led to a severe increase in the R/B values owing to the large difference in the averaged value between blue/green and pink channels. Exactly the same experiments shown in Fig. 6 were repeated as in Fig. S2 since the test solutions were prepared in CSF. The colorimetric responses and the results of digital imaging analysis shown in Fig. 6 were almost the same as those given in Fig. S6.

To evaluate the quantitative reliability of the colorimetric array, the Limit of Detection (LOD) and Limit of Quantitation (LOQ) were calculated based on the calibration curve derived from the 30 min detection data (pH 8), which were prioritized to demonstrate the method's rapid diagnostic capability. Using the standard deviation of the blank ($\sigma$ = 0.006) and the slope ($S = 9.00 \times 10^{-11}$), the LOD and LOQ were determined as $2.00 \times 10^{8}$ CFU mL$^{-1}$ and $6.67 \times 10^{8}$ CFU mL$^{-1}$, respectively ($R^2$ = 0.97), as detailed in Fig. S7 and Table S7 (SI). It is important to note that the sensitivity of this kinetic assay is time-dependent. As shown in Table S7, extending the incubation time to 90 min resulted in increased signal intensity, improving the theoretical LOD to $3.75 \times 10^{7}$ CFU mL$^{-1}$. However, for rapid clinical screening, the 30 min protocol provides the optimal balance between speed and precision. Also, kinetic analysis of the colorimetric array response over time for different bacterial concentrations is shown in Fig. S8.

As shown in Table S8, conventional culture-based workflows generally require longer response times and expert interpretation, whereas molecular and immunological methods provide faster readouts but typically require specialized infrastructure.[39–41] In this context, the proposed colorimetric array aims to offer a rapid, low-complexity alternative with an objective (optionally automated) readout.

To benchmark the proposed method against current technology, a detailed comparison with recently published optical biosensors (*e.g.*, SERS, fluorescence, and nanozymes) is provided in Table S9. While nanomaterial-based strategies achieve LODs suitable for trace analysis, they typically necessitate complex chemical synthesis and expensive instrumentation (*e.g.*, Raman spectrometers).[42–46] Crucially, although ultra-low detection limits are essential for screening asymptomatic carriers, acute bacterial meningitis is characterized clini-

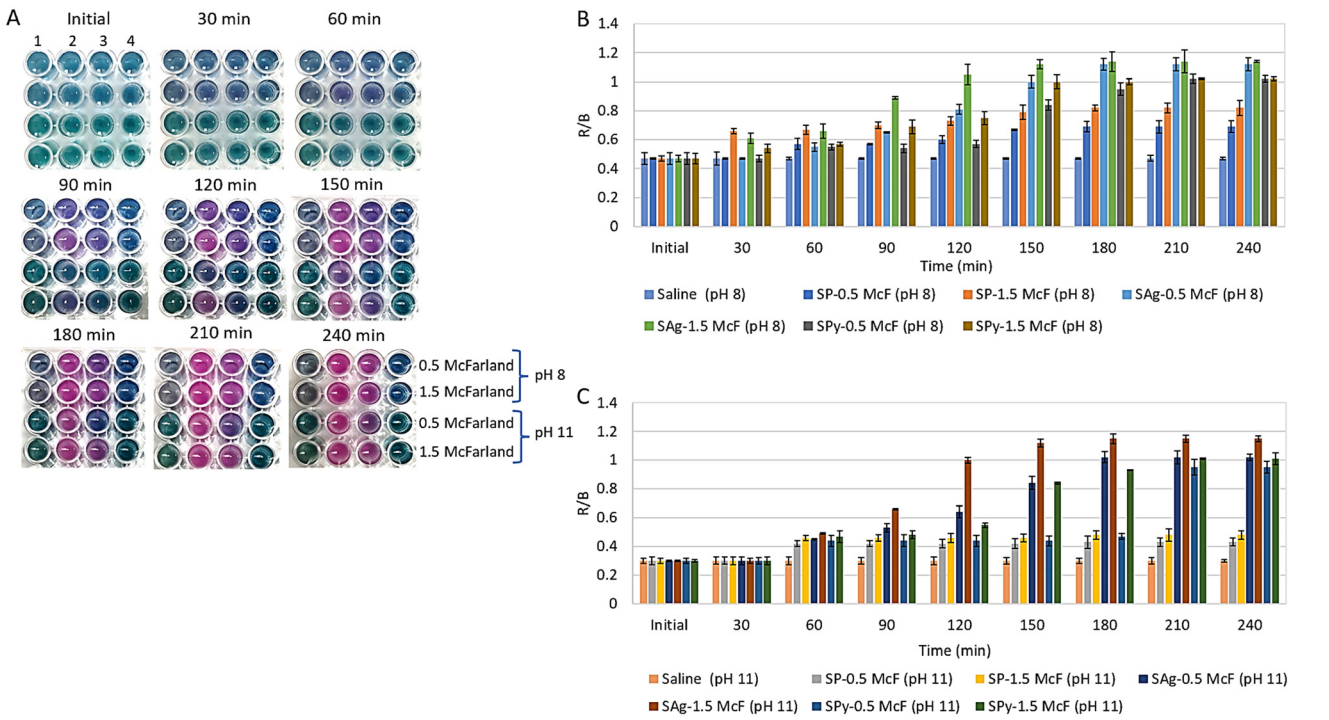


**Fig. 6** (A) Blue and green colorimetric arrays were prepared at pH 8 and pH 11 and incubated for different periods of time with different *Streptococcus* species in saline, (B) R/B analysis of the blue (pH 8) colorimetric array and (C) the green color (pH 11) colorimetric array (raw data provided in Tables S5 and S6). (Note: 0.5 and 1.5 McFarland correspond to $1.35 \times 10^{8}$ and $4.5 \times 10^{8}$ CFU mL$^{-1}$, respectively).

cally by high bacterial loads (titres) in the CSF.[47] Therefore, the sensitivity of the proposed colorimetric array is sufficient for its intended application of rapidly confirming active, high-burden infections. This approach deliberately prioritizes speed and accessibility over unnecessary ultra-sensitivity, addressing the urgent need for rapid diagnostics in resource-constrained acute care settings. Thus, our anthocyanin-based array prioritizes operational simplicity and cost-effectiveness, offering a rapid, instrument-free confirmation for acute infections without requiring proprietary substrates or specialized hardware.

### 3.1. Limitations and future perspectives

This proof-of-concept study has limitations. First, feasibility was demonstrated only in aCSF; patient-derived CSF (and other clinical matrices such as sputum) samples were not tested, and matrix-dependent interferences and any required pre-analytical processing therefore remain to be established. Because the readout is driven by $H_2O_2$-mediated oxidation, the apparent kinetics in real CSF may be influenced by endogenous redox-active components and enzymatic activities (*e.g.*, catalase/peroxidases), as well as occasional blood contamination, which can partially scavenge $H_2O_2$ and alter signal development. Accordingly, future studies will include a pilot clinical validation on ≥10 suspected infection samples (patient-derived CSF), using culture and/or molecular testing as comparators, to quantify matrix-interference effects and refine simple pre-analytical handling (*e.g.*, controlled dilution and removal of cells/debris where appropriate) to improve robustness. Second, we evaluated a single reference strain (*S. pneumoniae* ATCC 49619, serotype 19F) and did not assess performance across multiple serotypes and diverse clinical isolates; follow-up work will therefore benchmark a representative serotype panel and clinical isolates to quantify potential strain-to-strain variability in time-to-signal and detection limits. Finally, anthocyanins in aqueous solution may undergo gradual degradation depending on light, oxygen, temperature and pH, which can shift the baseline color during storage; future development will explore stabilized formats such as lyophilized (freeze-dried) reagents, pre-dosed kits or paper-based implementations to extend the shelf-life and improve portability. Coupling the assay with standardized smartphone imaging or miniaturized microfluidic platforms could further enable objective quantification and reduce user-to-user variability for point-of-care testing deployment.

## 4. Conclusions

In summary, we have developed anthocyanin-incorporated tests for rapid, sensitive and colorimetric detection of *S. pneumoniae* through the reaction mechanism of anthocyanin and $H_2O_2$. The $H_2O_2$ molecules released by *S. pneumoniae* are known as its virulence factor infecting or damaging host tissues. Anthocyanin, which is a biocompatible dye, is used as a major component in the test solution to provide colorimetric response in the presence of $H_2O_2$. *S. pneumoniae* colonizes in the lungs and produces $H_2O_2$ to protect themselves and causes bacterial pneumonia by stimulating an inflammatory response, and we uncovered the potential mechanism of detection of *S. pneumoniae*, in which released $H_2O_2$ molecules degrade anthocyanin molecules and induce a color change or color loss based on the concentration. As an ideal test solution, we used a test solution prepared using 5% anthocyanin at pH 8, with a blue color, and the blue color of the test solution turned into a gray color in 90 min after the addition of 1.5 McFarland *S. pneumoniae* suspension. The same concentration of *S. pneumoniae* was detected in 30 min using the image-processing software including R/B and Delta-E analysis, which showed enhanced detection sensitivity and speed for detecting *S. pneumoniae*. We claim that this *S. pneumoniae* detection tests can be implemented in the clinic and can provide onsite detection.

## Author contributions

C. C. Y.: conceptualization, methodology, investigation, project administration, writing – original draft, and writing – review & editing. N. T., N. I., P. S., M. A. A., A. Y., and E. G.: investigation, validation, and writing – review & editing. I. O.: conceptualization and writing – review & editing.

## Conflicts of interest

There are no conflicts to declare.

## Data availability

The data supporting this article have been included as part of the supplementary information (SI). Supplementary information: Fig. S1–S8 and Tables S1–S9. See DOI: https://doi.org/10.1039/d5an01356a.

## Acknowledgements

We would like to thank Yusuf Dogan for his assistance in drawing and designing.

## References

1 K. S. Ikuta, L. R. Swetschinski, G. R. Aguilar, F. Sharara, T. Mestrovic, S. S. Gray, N. D. Weaver, *et al.*, *Lancet*, 2022, **400**, 2221–2248.
2 C. Troeger, B. Blacker, I. A. Khalil, P. C. Rao, J. Cao, S. R. M. Zimsen, S. B. Albertson, J. D. Stanaway, *et al.*, *Lancet Infect. Dis.*, 2018, **18**, 1191–1210.
3 B. Ramos, N. K. Vadlamudi, C. Han and M. Sadarangani, *Lancet Infect. Dis.*, 2025, **25**(6), e330–e344.

4 Cleveland Clinic, Pneumococcal disease, https://my.clevelandclinic.org/health/diseases/24231-pneumococcal-disease, (accessed October 2025).
5 E. Womack, B. Alibayov, J. E. Vidal and Z. Eichenbaum, *Microbiol. Spectrum*, 2024, **12**, e03297-23.
6 H. Sati, E. Carrara, A. Savoldi, P. Hansen, J. Garlasco, E. Campagnaro and A. U. Nyaruhirira, *Lancet Infect. Dis.*, 2025, **5**(9), 1033–1043.
7 D. Chen, A. N. Schuetz and P. R. LaSala, *Clinical Pathology Board Review*, Elsevier, 2024, pp. 340.
8 L. Zhang, X. Xu, L. Cao, Z. Zhu, Y. Ding, H. Jiang, B. Li and J. Liu, *Microchim. Acta*, 2024, **191**, 29.
9 F. Mi, C. Hu, Y. Wang, T. Xu and J. P. Wu, *Anal. Bioanal. Chem.*, 2022, **414**, 2883–2902.
10 S. Liu, K. Zhao, M. Huang, S. Wang, Y. Zhang, Y. Wang and X. Zhang, *Front. Bioeng. Biotechnol.*, 2022, **10**, 958134.
11 X. Shkembi, V. Skouridou, M. Svobodova, G. Leonardo and C. K. O'Sullivan, *Anal. Chem.*, 2021, **93**, 14810–14819.
12 Q. Zhou, G. Zhang, Y. Wu, S. Wang and Y. Lu, *J. Am. Chem. Soc.*, 2023, **145**, 21370–21377.
13 O. Shelef, T. Kopp, R. Tannous, A. Shimon and Y. Shabat, *J. Am. Chem. Soc.*, 2024, **146**, 5263–5273.
14 C. W. Ma, K. K. H. Ng, B. H. C. Yam, Y. Wang and J. Wang, *J. Am. Chem. Soc.*, 2021, **143**, 6886–6894.
15 B. Klabunde, A. Wesener, W. Bertrams, K. Dierkes and B. Schmeck, *Cell Commun. Signaling*, 2023, **21**, 208.
16 P. Rai, M. Parrish, I. J. J. Tay, N. Li, S. Ackerman and Q. He, *Proc. Natl. Acad. Sci. U. S. A.*, 2015, **112**, E3421–E3430.
17 C. Celik Yoldas, N. Ildiz, P. Sagiroglu, M. A. Atalay, N. Y. Demir, M. Duman and I. Ocsoy, *Anal. Chem.*, 2025, **97**, 10619–10627.
18 C. Celik, N. Ildiz, M. Z. Kaya and I. Ocsoy, *Anal. Chim. Acta*, 2020, **1128**, 80–89.
19 C. Celik, N. Ildiz, P. Sagiroglu and I. Ocsoy, *Talanta*, 2020, **219**, 121292.
20 C. Celik, N. Y. Demir, M. Duman and I. Ocsoy, *Sci. Rep.*, 2023, **13**, 2056.
21 C. Celik, G. Kalin, Z. Cetinkaya and I. Ocsoy, *Diagnostics*, 2023, **13**, 2427.
22 N. Temur, E. Eryilmaz-Eren, I. Celik, I. E. Yildiz, M. Nisari, I. S. Unal, C. Celik and I. Ocsoy, *Smart Med.*, 2025, **4**, e70007.
23 C. Yilmaz, C. Celik, N. Ildiz and I. Ocsoy, in *Recent trends and advances in design of rapid tests for colorimetric detection of Staphylococcus aureus*, IntechOpen, 2024.
24 C. Celik, G. Can Sezgin, U. G. Kocabas and I. Ocsoy, *Anal. Chem.*, 2021, **93**, 6246–6253.
25 K. F. S. Alabbos, V. Jevtovic, J. Mitić and S. Mitić, *Processes*, 2025, **13**, 2245.
26 A. Venter, H. Fisher, G. I. Stafford and M. C. Taylor, *Int. J. Food Sci. Technol.*, 2022, **57**, 4347–4355.
27 S. M. Shalaby and H. H. Amin, *J. Probiotics Health*, 2018, **6**, 206.
28 X. Li, F. Wang, N. Ta and J. Liu, *Front. Plant Sci.*, 2025, **16**, 1544099.
29 Protocols.io, Preparation of recording ACSF (artificial cerebrospinal fluid), https://www.protocols.io/view/preparation-of-recording-acsf-artificial-cerebrosp-x54v9p4nmg3e/v1, (accessed October 2025).
30 D. J. Soldat, P. Barak and B. J. Lepore, *J. Chem. Educ.*, 2009, **86**, 617–620.
31 L. F. Capitán-Vallvey, N. López-Ruiz, A. Martínez-Olmos, M. M. Erenas and A. J. Palma, *Anal. Chim. Acta*, 2015, **899**, 23–56.
32 L. Gao, W. Ren, F. Li and H. M. Cheng, *ACS Nano*, 2008, **2**, 1625–1633.
33 V. Kılıc, G. Alankus, N. Horzum and M. T. Sezgin, *ACS Omega*, 2018, **3**, 5531–5536.
34 Y. Zhu, X. Zhang, J. Zhu and Y. Zhang, *Int. J. Mol. Sci.*, 2012, **13**, 12336–12348.
35 S. I. Siddiqui, E. S. Allehyani, S. A. Al-Harbi and I. Tyagi, *Processes*, 2023, **11**, 807.
36 R. Satake and E. Yanase, *Tetrahedron*, 2018, **74**, 6187–6191.
37 O. Dangles, *J. Agric. Food Chem.*, 2024, **72**, 12356–12372.
38 O. Dangles and J.-A. Fenger, *Molecules*, 2018, **23**, 1970.
39 S. S. Arbefeville, T. T. Timbrook and C. D. Garner, *J. Antimicrob. Chemother.*, 2024, **79**, i2–i8.
40 J. Contier, L. Platon, N. Benchabane, S. Tchakerian, F. Herman, C. Mollevi, P. Ceballos, S. Godreuil and K. Klouche, *Crit. Care*, 2025, **29**, 310.
41 S. Lee, J. S. Park, H. Woo, Y. K. Yoo, D. Lee, S. Chung, D. S. Yoon, K.-B. Lee and J. H. Lee, *Nat. Commun.*, 2024, **15**, 1695.
42 X. Cheng, X. Yang, Z. Tu, Z. Rong, C. Wang and S. Wang, *J. Hazard. Mater.*, 2023, **459**, 132192.
43 W. Shen, J. Li, B. Jiang, Y. Nie, Y. Pang, C. Wang, R. Xiao and R. Hao, *Pathogens*, 2023, **12**, 327.
44 X. Jia, Z. Liu, J. Zhou, C. Cao, Y. Hao, J. Chen, H. Han, J. Liang, Z. Zhao, Y. Wang, Z. Niu and R. Xiao, *Nanomedicine*, 2025, **69**, 102853.
45 G. Goikoetxea, K.-T. K. Akhtar, A. Prysiazhniuk, B. A. Borsa, M. E. Aldag, M. Kavruk, V. C. Ozalp and F. J. Hernandez, *Analyst*, 2024, **149**, 1289–1296.
46 Y. Guo, Z. Tu, H. Chen, H. Wei, T. Wang, G. Sun and Z. Rong, *Analyst*, 2026, **151**, 830–841.
47 N. Chekrouni, T. M. van Soest, A. C. da Cruz Campos, M. C. Brouwer and D. van de Beek, *Clin. Microbiol. Infect.*, 2024, **30**, 772–778.